2021 American Control Conference (ACC)
New Orleans, USA, May 25-28, 2021

Singularity-Free Decentralized Formation Tracking Control for Heterogeneous Underactuated Surface Vessels*

Bo Wang, Sergey Nersesov, and Hashem Ashrafiuon

Abstract— **This paper presents a decentralized leader-following formation tracking control framework for heterogeneous underactuated surface vessels with a directed communication topology. Our design relies only on the assumption that either yaw or surge reference velocity is persistently exciting. First, each vessel in the network is modeled as a generic planar rigid body with two control inputs using the appropriate kinematic and force-balance equations. We take advantage of the cascade structure of the combined kinematic and dynamic model of surface vessels and develop a reduced-order error dynamics. Then, a smooth time-varying controller is developed with the aid of Lyapunov method. The proposed controller guarantees the uniform global asymptotic stability and strong robustness properties in the formation-error-coordinates space. In our approach, formation is achieved without global position measurements and the vessels may have heterogeneous dynamic models. Furthermore, the formation tracking problem for underactuated surface vessels is solved without any singularity conditions. Simulation results are provided to validate the proposed control framework.**

I. INTRODUCTION

For a group of autonomous vehicles, the formation control problem roughly consists of driving multiple vehicles to achieve and stay in a predefined spatial configuration and move along a reference trajectory. Research on formation control of surface vessel networks has grown overwhelmingly over the past decade in marine industry since it has many applications in practice such as reconnaissance, marine search and rescue missions, and mine clearance, to name a few. Various approaches to formation control of autonomous vehicles have been proposed, for instance, using leader-following strategy [1], behavior-based method [2], and virtual structure approach [3]. Among these schemes, leader-following strategy is particularly appreciated in many applications for its simplicity and scalability [4].

Leader-following formation control of underactuated surface vessels has been addressed by control community starting, at least, with [1] in which sliding mode formation controllers have been proposed for surface vessels based on two specific geometric communication network topology schemes. In [5], cooperative control laws have been proposed for underactuated surface vessels to solve the formation stabilization problem. In [6], position-based control laws have been proposed to solve the formation tracking problem for underactuated surface vessels under the assumption that the yaw reference velocity of leader is persistently exciting (PE). In [7], centralized cooperative control laws gave been presented for underactuated vessels with limited sensing ranges to perform a desired formation and guarantee no collisions between the vessels. In [8], using time-varying tan-type barrier Lyapunov functions, a fault tolerant formation control scheme was proposed for a class of underactuated surface vessels with line-of-sight range and angle constraints. This work was extended in [9] to asymmetric time-varying constraints on the range and bearing angle between the follower and the leader in the formation. In [10], based on sliding mode control and parameter estimation, formation control laws have been proposed for surface vehicles with model uncertainties and environmental disturbances. In [11], the authors presented a finite-time formation controller for underactuated ships based on terminal sliding mode theory.

However, there are several common drawbacks in the previous formation designs. Firstly, from a practical viewpoint, the surface vessels in the network may own different parameters or dynamics due to the various sizes and overloads. Therefore, it is useful if a group of vessels can cooperate with each other regardless of the parameters or even structures of their dynamic models. In [1], [5], [6], [9], [11], not only the dynamics, but also the parameters of all the vessels in the network are required to be identical, which is a very strict assumption. Furthermore, using global sensors could be a quite demanding requirement depending upon environment and could be biased easily due to measurement errors. Thus, to improve the cooperative ability, traffic safety and communication efficiency, it is required to have vessel-to-vessel interactions, and to control the inter-vessel configurations with onboard vehicle sensors. Moreover, for tracking control of underactuated surface vessels, it is common to require that the desired trajectory satisfies certain singularity conditions such as PE of yaw velocity [6], or yaw velocity separating from zero [12], [13], [14]. In this case, the singularity conditions impose strict requirements on the reference trajectories so that the vessel cannot even track a straight line. For formation control of nonholonomic mobile robots, various control schemes have been proposed, for example, to solve the problems of heterogeneity [15], the singularity conditions [16], and decentralized design [17]. However, due to the underactuation and the specific dynamics of surface vessels, it is difficult to extend these control designs to underactuated vessels.

The main contribution and novelty of this paper is to present a singularity-free decentralized leader-following formation control framework for heterogeneous underactuated

*This research was supported in part by the U.S. Office of Naval Research under Grant N00014-19-1-2255.

Bo Wang, Sergey Nersesov, and Hashem Ashrafiuon are with the Department of Mechanical Engineering, Villanova University, Villanova, PA, USA. Email: {bwang6, sergey.nersesov, hashem.ashrafiuon}@villanova.edu.

surface vessels with a directed communication topology. Our design relies upon the assumption that *either* the yaw *or* the surge reference velocity is persistently exciting; i.e. the only requirement is for the vessel to be moving. First, each vessel in the network is modeled as a generic planar rigid body with two control inputs using the appropriate kinematic and force-balance equations. We take advantage of the cascade structure of the combined kinematic and dynamic model of surface vessels and develop a reduced-order error dynamics. Then, an smooth time-varying controller is developed with the aid of Lyapunov method. The proposed controller guarantees the uniform global asymptotic stability and strong robustness properties in the formation-error-coordinates space, and can be implemented in directed time-invariant communication networks with a spanning tree. Compared with existing methods, the formation is achieved without global position measurements and the vessels in the network are allowed to have different dynamics. Furthermore, our approach solves the formation tracking problem for underactuated surface vessels without introducing any singularity conditions.

The rest of the paper is organized as follows. Section II presents the preliminaries and problem formulation. The transformation to reduce the order of error dynamics and the formation control design are proposed in Section III. Simulation examples are shown in Section IV to verify the theoretical results. Finally, the concluding remarks are presented in Section V.

II. Preliminaries and Problem Formulation

A. Model Description

Consider a group of $N+1$ heterogeneous underactuated surface vessels where the vessels are indexed $\mathbf{i}=0,1,\dots,N$ with $\mathbf{0}$ representing the leader vessel and $\mathbf{1},\dots,\mathbf{N}$ representing the followers. The configuration of each vessel can be described by a vector of generalized coordinates $q_\mathbf{i}=[x_\mathbf{i},y_\mathbf{i},\theta_\mathbf{i}]^\top$, where $(x_\mathbf{i},y_\mathbf{i})$ is the position of the vessel $\mathbf{i}$ in the global coordinate system $\{XY\}$, and $\theta_\mathbf{i}$ is the heading angle, as shown in Fig. 1. We assume that each vessel has only two actuators, which provide the surge control force and the yaw control moment. Under this assumption, the motion of the surface vessel $\mathbf{i}$ is described by the following equations [14]

$$\begin{cases} \dot{x}_\mathbf{i}=v_{x\mathbf{i}}\cos\theta_\mathbf{i}-v_{y\mathbf{i}}\sin\theta_\mathbf{i},\\ \dot{y}_\mathbf{i}=v_{x\mathbf{i}}\sin\theta_\mathbf{i}+v_{y\mathbf{i}}\cos\theta_\mathbf{i},\\ \dot{\theta}_\mathbf{i}=\omega_\mathbf{i}, \end{cases} \tag{1a}$$

$$\begin{cases} \dot{v}_{x\mathbf{i}}=f_{x\mathbf{i}}(v_{x\mathbf{i}},v_{y\mathbf{i}},\omega_\mathbf{i})+\delta_{x\mathbf{i}}(v_{x\mathbf{i}},v_{y\mathbf{i}},\omega_\mathbf{i},t)+\tau_{1\mathbf{i}},\\ \dot{v}_{y\mathbf{i}}=f_{y\mathbf{i}}(v_{x\mathbf{i}},v_{y\mathbf{i}},\omega_\mathbf{i})+\delta_{y\mathbf{i}}(v_{x\mathbf{i}},v_{y\mathbf{i}},\omega_\mathbf{i},t),\\ \dot{\omega}_\mathbf{i}=f_{\omega\mathbf{i}}(v_{x\mathbf{i}},v_{y\mathbf{i}},\omega_\mathbf{i})+\delta_{\omega\mathbf{i}}(v_{x\mathbf{i}},v_{y\mathbf{i}},\omega_\mathbf{i},t)+\tau_{2\mathbf{i}}, \end{cases} \tag{1b}$$

where $(v_{x\mathbf{i}},v_{y\mathbf{i}})$ represents the velocity of the center of mass of vehicle $\mathbf{i}$ in the body-fixed frame $\{x_{b\mathbf{i}}y_{b\mathbf{i}}\}$ and $\omega_\mathbf{i}$ is its angular velocity. The velocity vector is denote by $v_\mathbf{i}=[v_{x\mathbf{i}},v_{y\mathbf{i}},\omega_\mathbf{i}]^\top$. $f_{x\mathbf{i}}(\cdot),f_{y\mathbf{i}}(\cdot),f_{\omega\mathbf{i}}(\cdot)$ are known locally Lipschitz continuous functions which usually consist of Coriolis and centrifugal and hydrodynamic damping terms. The terms

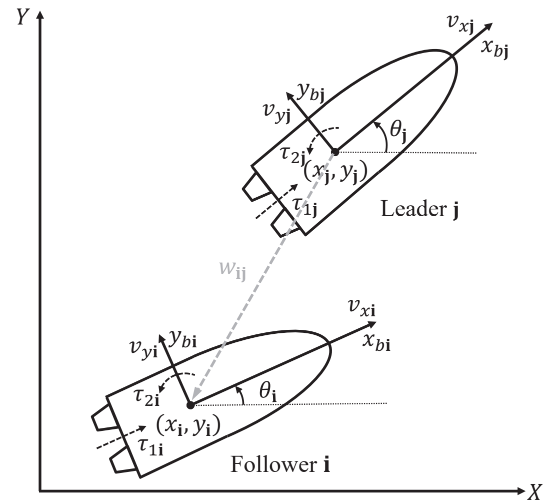

Fig. 1. Top view of the leader-follower formation of underactuated surface vessels $\mathbf{i}$ and $\mathbf{j}$.

$\delta_{x\mathbf{i}}(\cdot),\delta_{y\mathbf{i}}(\cdot),\delta_{\omega\mathbf{i}}(\cdot)$ represent the unknown but bounded modeling uncertainties and disturbances, i.e.,

$$|\delta_{x\mathbf{i}}(\cdot)|_\infty\le\Delta_{x\mathbf{i}},\ \ |\delta_{y\mathbf{i}}(\cdot)|_\infty\le\Delta_{y\mathbf{i}},\ \ |\delta_{\omega\mathbf{i}}(\cdot)|_\infty\le\Delta_{\omega\mathbf{i}},$$

where $\Delta_{x\mathbf{i}},\Delta_{y\mathbf{i}},\Delta_{\omega\mathbf{i}}$ are known positive constants. $\tau_{1\mathbf{i}}$ and $\tau_{2\mathbf{i}}$ are the scaled control inputs representing the surge force and yaw moment, respectively, as shown in Fig. 1.

From the planar kinetics of rigid bodies, the term $f_{y\mathbf{i}}(\cdot)$ in the sway force-balance equation in (1b) consists of quadratic Coriolis and centrifugal force terms $f^{\mathsf{C}}_{y\mathbf{i}}(\cdot)$ and damping terms $f^{\mathsf{D}}_{y\mathbf{i}}(\cdot)$, that is $f_{y\mathbf{i}}=f^{\mathsf{C}}_{y\mathbf{i}}+f^{\mathsf{D}}_{y\mathbf{i}}$. From rigid bodies mechanics, the Coriolis force has the form $-2m_\mathbf{i}\vec{\omega}_\mathbf{i}\times\vec{v}_\mathbf{i}$, and the centrifugal force has the form $-m_\mathbf{i}\vec{\omega}_\mathbf{i}\times(\vec{\omega}_\mathbf{i}\times\vec{r}_\mathbf{i})$, which implies that the components of Coriolis and centrifugal forces in $y_{b\mathbf{i}}$ direction are only functions of $v_{x\mathbf{i}}$ and $\omega_\mathbf{i}$, that is $f^{\mathsf{C}}_{y\mathbf{i}}=f^{\mathsf{C}}_{y\mathbf{i}}(v_{x\mathbf{i}},\omega_\mathbf{i})$, and the directions of the forces are opposite to the $y_{b\mathbf{i}}$ direction. Furthermore, the component of the hydrodynamic damping force in the direction $y_{b\mathbf{i}}$ is only related to $v_{y\mathbf{i}}$, that is $f^{\mathsf{D}}_{y\mathbf{i}}=f^{\mathsf{D}}_{y\mathbf{i}}(v_{y\mathbf{i}})$, and its direction is opposite to the direction of $v_{y\mathbf{i}}$. Based on the above discussion, we make the following assumption.

Assumption 1: The term $f_{y\mathbf{i}}(\cdot)$ in the sway force-balance equation in (1b) are given by

$$f_{y\mathbf{i}}(v_{x\mathbf{i}},v_{y\mathbf{i}},\omega_\mathbf{i})=f^{\mathsf{C}}_{y\mathbf{i}}(v_{x\mathbf{i}},\omega_\mathbf{i})+f^{\mathsf{D}}_{y\mathbf{i}}(v_{y\mathbf{i}}) \tag{2}$$

with the Coriolis and centrifugal terms $f^{\mathsf{C}}_{y\mathbf{i}}(v_{x\mathbf{i}},\omega_\mathbf{i})$ satisfying

$$\frac{\partial f^{\mathsf{C}}_{y\mathbf{i}}}{\partial v_{x\mathbf{i}}}(v_{x\mathbf{i}}(t),\omega_\mathbf{i}(t))=-\eta_\mathbf{i}\omega_\mathbf{i}(t),\ \ \forall t\ge 0, \tag{3}$$

where $\eta_\mathbf{i}>0$ is a constant related to the inertia parameters, and the hydrodynamic damping term $f^{\mathsf{D}}_{y\mathbf{i}}(v_{y\mathbf{i}})$ satisfying

$$\frac{\partial f^{\mathsf{D}}_{y\mathbf{i}}}{\partial v_{y\mathbf{i}}}(v_{y\mathbf{i}}(t))\le 0,\ \ \forall t\ge 0. \tag{4}$$

Remark 1: The Assumption 1 is realistic from the physics of the problem. Actually, the generic vessel model (1a), (1b) with Assumption 1 covers most vessel models in practical applications such as models presented in the works [12], [18], [19]. Furthermore, as pointed in [20], since the hydrodynamic damping forces in the $v_{y\mathbf{i}}$-equation are dominant in the sway direction, the sway velocity of the surface vessel is passive bounded, and thus it is uniformly ultimately bounded [20]. Moreover, clearly, the model (1a), (1b) is underactuated since there is no sway control force in the $v_{y\mathbf{i}}$-equation in (1b).

B. Preliminaries of Graph Theory

For formation control of surface vessels, we use graph theory to define the communication network among the vessels. Network topology of the $N+1$ surface vessels is defined by a directed graph $\mathscr{G}=(\mathscr{V},\mathscr{E})$ where $\mathscr{V}$ and $\mathscr{E}\subseteq\mathscr{V}\times\mathscr{V}$ represent its sets of vertices and edges, respectively. There are $N+1$ nodes whose node dynamics are described in (1a), (1b). The set of neighboring nodes with edges connected to node $\mathbf{i}$ is denoted by $\Omega_{\mathbf{i}}=\{\mathbf{j}\mid(\mathbf{i},\mathbf{j})\in\mathscr{E}\}$. The edges represent communication between the nodes such that (follower) node $\mathbf{i}$ can obtain information from (leader) node $\mathbf{j}$ for feedback control purposes, if $\mathbf{j}\in\Omega_{\mathbf{i}}$, as shown in Fig. 1. In order to incorporate a combination of neighboring feedback information from neighboring nodes, we let $w_{\mathbf{ij}}\geq 0$ be a constant weighing factor for any $\mathbf{i},\mathbf{j}\in\mathscr{V}$. These factors are selected such that $\sum_{\mathbf{j}\in\Omega_{\mathbf{i}}}w_{\mathbf{ij}}=1$ if $(\mathbf{i},\mathbf{j})\in\mathscr{E}$ and $w_{\mathbf{ij}}=0$, otherwise. We assume that there exists at least one directed path starting from the leader $\mathbf{0}$ to any other node in the network, which implies that the graph $\mathscr{G}$ is weakly connected. Furthermore, we assume that the communication topology is time invariant, there are no self-loops in the graph, and the leader does not receive any communication from other nodes.

C. Problem Formulation

Consider $N+1$ heterogeneous underactuated surface vessels with a communication network described by a directed graph $\mathscr{G}$. The objective of leader-follower formation control is to design a *decentralized* controller such that the follower agents move together according to the leader's motion and asymptotically converge to a desired geometric pattern. The desired position geometric pattern of the network of vessels may be defined by a set of constant position offset vectors $\{(d^1_{\mathbf{ij}},d^2_{\mathbf{ij}})\in\mathbb{R}^2:\mathbf{i},\mathbf{j}\in\mathscr{V},\,\mathbf{i}\neq\mathbf{j}\}$. More precisely, the following formation control problem is addressed in this paper.

Formation control problem. Without global position measurements of follower agents, design control laws $\tau_{1\mathbf{i}},\tau_{2\mathbf{i}}$ for the $\mathbf{i}$-th follower such that: (i) all the signals in the closed-loop system are uniformly bounded; (ii) all the vessels in the network can maintain a prescribed formation position in the sense that

$$\lim_{t\to\infty}\left|\begin{bmatrix}x_{\mathbf{i}}(t)-x_{\mathbf{j}}(t)-d^1_{\mathbf{ij}}\\ y_{\mathbf{i}}(t)-y_{\mathbf{j}}(t)-d^2_{\mathbf{ij}}\end{bmatrix}\right|=0,\quad\forall\,\mathbf{i},\mathbf{j}\in\mathscr{V}. \tag{5}$$

It follows from Lemma 3.3 in [17] that the formation objective (5) holds if and only if the following equation holds:

$$\lim_{t\to\infty}\left|\begin{bmatrix}x_{\mathbf{i}}(t)\\ y_{\mathbf{i}}(t)\end{bmatrix}-\sum_{\mathbf{j}\in\Omega_{\mathbf{i}}}w_{\mathbf{ij}}\begin{bmatrix}x_{\mathbf{j}}(t)+d^1_{\mathbf{ij}}\\ y_{\mathbf{j}}(t)+d^2_{\mathbf{ij}}\end{bmatrix}\right|=0,\ \forall\,\mathbf{i}=1,\ldots,N. \tag{6}$$

Remark 2: In marine practice of the formation control of surface vehicles, the position offset vector may be smooth time-varying vectors $(d^1_{\mathbf{ij}}(t),d^2_{\mathbf{ij}}(t))$ instead of constant vectors and in this case the formation is time-varying. Although in this paper we focus on time invariant formation, all the results in this paper can be easily generalized to the case of time-varying formations. This, however, is omitted in our discussion to simplify the notation and derivations.

We make the following assumption on the leader vessel $\mathbf{0}$.

Assumption 2: The state variable of the leader vessel $(q_{\mathbf{0}},v_{\mathbf{0}})$ and its first derivative are bounded for all $t\geq 0$. In addition, *either* the surge velocity *or* the yaw velocity of the leader is PE, that is, there exist $T,\mu>0$ such that

$$\int_t^{t+T}\left(|v_{x\mathbf{0}}(s)|+|\omega_{\mathbf{0}}(s)|\right)\mathrm{d}s\geq\mu,\ \ \forall t\geq 0. \tag{7}$$

D. Feasible Reference Trajectories Generation

Due to the underactuation nature of surface vehicles, the reference configuration trajectory dictated by the formation cannot be assigned arbitrarily to vessel $\mathbf{i}$. In other words, given the relative position measurements $\{(x_{\mathbf{i}}(t)-x_{\mathbf{j}}(t),y_{\mathbf{i}}(t)-y_{\mathbf{j}}(t)):\mathbf{j}\in\Omega_{\mathbf{i}}\}$ and the desired formation position offset vectors $\{(d^1_{\mathbf{ij}},d^2_{\mathbf{ij}}):\mathbf{j}\in\Omega_{\mathbf{i}}\}$ for vessel $\mathbf{i}$, the feasible orientation trajectory must be determined based on the vessel model. More precisely, let us denote the position reference trajectory for the vessel $\mathbf{i}$ by

$$\begin{aligned}\bar{x}_{\mathbf{i}}(t)&:=\sum_{\mathbf{j}\in\Omega_{\mathbf{i}}}w_{\mathbf{ij}}\left(x_{\mathbf{j}}(t)+d^1_{\mathbf{ij}}\right),\\ \bar{y}_{\mathbf{i}}(t)&:=\sum_{\mathbf{j}\in\Omega_{\mathbf{i}}}w_{\mathbf{ij}}\left(y_{\mathbf{j}}(t)+d^2_{\mathbf{ij}}\right).\end{aligned} \tag{8}$$

Then, the feasible orientation trajectory defined by

$$\bar{\theta}_{\mathbf{i}}(t):=\sum_{\mathbf{j}\in\Omega_{\mathbf{i}}}w_{\mathbf{ij}}\left(\theta_{\mathbf{j}}(t)+d^3_{\mathbf{ij}}\right) \tag{9}$$

is forced to obey the same second-order nonholonomic constraint as the vessel $\mathbf{i}$, where $d^3_{\mathbf{ij}}$ denotes the desired orientation offset. Then, the reference configuration trajectory $\bar{q}_{\mathbf{i}}(t):=[\bar{x}_{\mathbf{i}}(t),\bar{y}_{\mathbf{i}}(t),\bar{\theta}_{\mathbf{i}}(t)]^\top$ can be seen as one generated by a virtual system subjected to the same constraints as the vessel $\mathbf{i}$:

$$\begin{cases}\dot{\bar{x}}_{\mathbf{i}}(t)=\bar{v}_{x\mathbf{i}}(t)\cos\bar{\theta}_{\mathbf{i}}(t)-\bar{v}_{y\mathbf{i}}(t)\sin\bar{\theta}_{\mathbf{i}}(t),\\ \dot{\bar{y}}_{\mathbf{i}}(t)=\bar{v}_{x\mathbf{i}}(t)\sin\bar{\theta}_{\mathbf{i}}(t)+\bar{v}_{y\mathbf{i}}(t)\cos\bar{\theta}_{\mathbf{i}}(t),\\ \dot{\bar{\theta}}_{\mathbf{i}}(t)=\bar{\omega}_{\mathbf{i}}(t),\end{cases} \tag{11a}$$

$$\begin{cases}\dot{\bar{v}}_{x\mathbf{i}}(t)=f_{x\mathbf{i}}\left(\bar{v}_{x\mathbf{i}}(t),\bar{v}_{y\mathbf{i}}(t),\bar{\omega}_{\mathbf{i}}(t)\right)+\bar{\tau}_{1\mathbf{i}}(t),\\ \dot{\bar{v}}_{y\mathbf{i}}(t)=f_{y\mathbf{i}}\left(\bar{v}_{x\mathbf{i}}(t),\bar{v}_{y\mathbf{i}}(t),\bar{\omega}_{\mathbf{i}}(t)\right),\\ \dot{\bar{\omega}}_{\mathbf{i}}(t)=f_{\omega\mathbf{i}}\left(\bar{v}_{x\mathbf{i}}(t),\bar{v}_{y\mathbf{i}}(t),\bar{\omega}_{\mathbf{i}}(t)\right)+\bar{\tau}_{2\mathbf{i}}(t),\end{cases} \tag{11b}$$

where $\bar{v}_{\mathbf{i}}(t):=[\bar{v}_{x\mathbf{i}}(t),\bar{v}_{y\mathbf{i}}(t),\bar{\omega}_{\mathbf{i}}(t)]^\top$ is the reference velocity vector assigned by all vessels $\mathbf{j}\in\Omega_{\mathbf{i}}$, and $\bar{\tau}_{1\mathbf{i}}(t),\bar{\tau}_{2\mathbf{i}}(t)$ are the corresponding desired virtual control inputs. As proposed in [14], the feasible orientation trajectory $\bar{\theta}_{\mathbf{i}}(t)$ is a solution to the following first order ordinary differential equation (ODE):

$$\dot{\bar{v}}_{y\mathbf{i}}(t) = f_{y\mathbf{i}}\left(\bar{v}_{x\mathbf{i}}(t), \bar{v}_{y\mathbf{i}}(t), \dot{\bar{\theta}}_{\mathbf{i}}(t)\right), \tag{12}$$

subject to the initial condition $\bar{\theta}_{\mathbf{i}}(0) = \bar{\theta}_{\mathbf{i},0}$, where $\bar{v}_{x\mathbf{i}}(t)$ and $\bar{v}_{y\mathbf{i}}(t)$ are given by

$$\begin{aligned} \bar{v}_{x\mathbf{i}}(t) &= \cos\bar{\theta}_{\mathbf{i}}(t)\dot{\bar{x}}_{\mathbf{i}}(t) + \sin\bar{\theta}_{\mathbf{i}}(t)\dot{\bar{y}}_{\mathbf{i}}(t), \\ \bar{v}_{y\mathbf{i}}(t) &= -\sin\bar{\theta}_{\mathbf{i}}(t)\dot{\bar{x}}_{\mathbf{i}}(t) + \cos\bar{\theta}_{\mathbf{i}}(t)\dot{\bar{y}}_{\mathbf{i}}(t), \end{aligned} \tag{13}$$

and $\bar{x}_{\mathbf{i}}(t), \bar{y}_{\mathbf{i}}(t)$ are given by (8). Therefore, the feasible orientation trajectory $\bar{\theta}_{\mathbf{i}}(t)$ is calculated by numerically integrating(12) given the reference position offset vectors $\{(d^1_{\mathbf{ij}}, d^2_{\mathbf{ij}}) : \mathbf{j} \in \Omega_{\mathbf{i}}\}$. Finally, the feasible orientation offset $d^3_{\mathbf{ij}}$ is selected as $d^3_{\mathbf{ij}} = \bar{\theta}_{\mathbf{i}}(t) - \theta_{\mathbf{j}}(t)$.

III. Control Design and Main Results

A. Error Dynamics

The objective of formation control of surface vessels is to achieve $|q_{\mathbf{i}}(t) - \bar{q}_{\mathbf{i}}(t)| \to 0$ and $|v_{\mathbf{i}}(t) - \bar{v}_{\mathbf{i}}(t)| \to 0$ as $t \to \infty$. For this problem, we usually calculate the dynamics of the formation error $(\tilde{q}_{\mathbf{i}}, \tilde{v}_{\mathbf{i}}) := (q_{\mathbf{i}} - \bar{q}_{\mathbf{i}}, v_{\mathbf{i}} - \bar{v}_{\mathbf{i}})$ and convert the formation control problem into one of stabilization of the error system. However, due to the underactuation, the error dynamics often becomes complicated and hard to stabilize. To achieve the formation objective (6), note that the vessel model (1a), (1b) has a cascade structure of the kinematics and kinetics. Therefore, we define the formation error vector $z_{\mathbf{i}} = [z_{1\mathbf{i}}, z_{2\mathbf{i}}, z_{3\mathbf{i}}]^\top$ for agents $\mathbf{i}$ using the following transformation:

$$z_{\mathbf{i}} = J(\theta_{\mathbf{i}})\left[(\dot{q}_{\mathbf{i}} - \dot{\bar{q}}_{\mathbf{i}}) + \Lambda(q_{\mathbf{i}} - \bar{q}_{\mathbf{i}})\right], \tag{14}$$

where $J(\theta_{\mathbf{i}})$ is the orthogonal rotation matrix

$$J(\theta_{\mathbf{i}}) := \begin{bmatrix} \cos\theta_{\mathbf{i}} & \sin\theta_{\mathbf{i}} & 0 \\ -\sin\theta_{\mathbf{i}} & \cos\theta_{\mathbf{i}} & 0 \\ 0 & 0 & 1 \end{bmatrix}, \tag{15}$$

and $\Lambda = \mathrm{diag}\{\lambda_1, \lambda_2, \lambda_3\}$ is a diagonal and positive definite matrix. We have the following results.

Lemma 1: Consider the formation error $z_{\mathbf{i}}$ defined in (14), where $\Lambda = \mathrm{diag}\{\lambda_1, \lambda_2, \lambda_3\}$ is a positive definite matrix. For any agent $\mathbf{i} = 1, \ldots, N$, if the error $z_{\mathbf{i}}(t)$ is bounded for all $t \geq 0$, and $z_{\mathbf{i}} \to 0$ as $t \to \infty$, then the formation tracking problem defined by (5) is solved.

Proof: Since $J(\theta_{\mathbf{i}})$ is orthogonal matrix, $z_{\mathbf{i}} \in \mathscr{L}_\infty$ implies $[(\dot{q}_{\mathbf{i}} - \dot{\bar{q}}_{\mathbf{i}}) + \Lambda(q_{\mathbf{i}} - \bar{q}_{\mathbf{i}})] \in \mathscr{L}_\infty$, and $z_{\mathbf{i}} \to 0$ implies $[(\dot{q}_{\mathbf{i}} - \dot{\bar{q}}_{\mathbf{i}}) + \Lambda(q_{\mathbf{i}} - \bar{q}_{\mathbf{i}})] \to 0$, which may be written as

$$\frac{\mathrm{d}}{\mathrm{d}t}(q_{\mathbf{i}} - \bar{q}_{\mathbf{i}}) = -\Lambda(q_{\mathbf{i}} - \bar{q}_{\mathbf{i}}) + o_{\mathbf{i}}(t), \quad \lim_{t\to\infty} o_{\mathbf{i}}(t) = 0, \tag{16}$$

where $o_{\mathbf{i}}(t) = J(\theta_{\mathbf{i}})^\top z_{\mathbf{i}}(t)$. Then from the converging-input convergent-state (CICS) property of stable linear systems [21], we conclude that $(q_{\mathbf{i}} - \bar{q}_{\mathbf{i}})$ is bounded and $(q_{\mathbf{i}} - \bar{q}_{\mathbf{i}}) \to 0$ as $t \to \infty$. Since this convergence holds for all $\mathbf{i} = 1, \ldots, N$, we can conclude that (6) and consequently (5) hold. □

Referring to Lemma 1, the objective of formation control design is to drive $z_{\mathbf{i}}$, $\mathbf{i} = 1, \ldots, N$ to zero asymptotically. The error dynamics in terms of $z_{\mathbf{i}}$ is determined by taking the time derivative of (14):

$$\begin{aligned} \dot{z}_{\mathbf{i}} &= \dot{J}\left[(\dot{q}_{\mathbf{i}} - \dot{\bar{q}}_{\mathbf{i}}) + \Lambda(q_{\mathbf{i}} - \bar{q}_{\mathbf{i}})\right] + J\left[(\ddot{q}_{\mathbf{i}} - \ddot{\bar{q}}_{\mathbf{i}}) + \Lambda(\dot{q}_{\mathbf{i}} - \dot{\bar{q}}_{\mathbf{i}})\right] \\ &= \begin{bmatrix} \omega_{\mathbf{i}} z_{2\mathbf{i}} \\ -\omega_{\mathbf{i}} z_{1\mathbf{i}} \\ 0 \end{bmatrix} + J(\theta_{\mathbf{i}})\ddot{q}_{\mathbf{i}} - J(\theta_{\mathbf{i}})\ddot{\bar{q}}_{\mathbf{i}} + \Lambda v_{\mathbf{i}} - \Lambda J(\theta_{\mathbf{i}})\dot{\bar{q}}_{\mathbf{i}} \\ &= \begin{bmatrix} \omega_{\mathbf{i}} z_{2\mathbf{i}} \\ -\omega_{\mathbf{i}} z_{1\mathbf{i}} \\ 0 \end{bmatrix} + \begin{bmatrix} \dot{v}_{x\mathbf{i}} - \omega_{\mathbf{i}} v_{y\mathbf{i}} - c_{(\mathbf{i}-\bar{\mathbf{i}})}\left(\dot{\bar{v}}_{x\mathbf{i}} - \bar{\omega}_{\mathbf{i}}\bar{v}_{y\mathbf{i}}\right) - s_{(\mathbf{i}-\bar{\mathbf{i}})}\left(\dot{\bar{v}}_{y\mathbf{i}} + \bar{\omega}_{\mathbf{i}}\bar{v}_{x\mathbf{i}}\right) + \lambda_1\left(v_{x\mathbf{i}} - c_{(\mathbf{i}-\bar{\mathbf{i}})}\bar{v}_{x\mathbf{i}} - s_{(\mathbf{i}-\bar{\mathbf{i}})}\bar{v}_{y\mathbf{i}}\right) \\ \dot{v}_{y\mathbf{i}} + \omega_{\mathbf{i}} v_{x\mathbf{i}} + s_{(\mathbf{i}-\bar{\mathbf{i}})}\left(\dot{\bar{v}}_{x\mathbf{i}} - \bar{\omega}_{\mathbf{i}}\bar{v}_{y\mathbf{i}}\right) - c_{(\mathbf{i}-\bar{\mathbf{i}})}\left(\dot{\bar{v}}_{y\mathbf{i}} + \bar{\omega}_{\mathbf{i}}\bar{v}_{x\mathbf{i}}\right) + \lambda_2\left(v_{y\mathbf{i}} + s_{(\mathbf{i}-\bar{\mathbf{i}})}\bar{v}_{x\mathbf{i}} - c_{(\mathbf{i}-\bar{\mathbf{i}})}\bar{v}_{y\mathbf{i}}\right) \\ \dot{\omega}_{\mathbf{i}} - \dot{\bar{\omega}}_{\mathbf{i}} + \lambda_3(\omega_{\mathbf{i}} - \bar{\omega}_{\mathbf{i}}) \end{bmatrix}, \end{aligned} \tag{17}$$

where $c_{(\mathbf{i}-\bar{\mathbf{i}})} := \cos(\theta_{\mathbf{i}} - \bar{\theta}_{\mathbf{i}})$, and $s_{(\mathbf{i}-\bar{\mathbf{i}})} := \sin(\theta_{\mathbf{i}} - \bar{\theta}_{\mathbf{i}})$. Substituting (1a), (1b), (11a) and (11b) into (17), and using the feedback transformations

$$\begin{aligned} \tau_{1\mathbf{i}} &= u_{1\mathbf{i}} + \omega_{\mathbf{i}} v_{y\mathbf{i}} + c_{(\mathbf{i}-\bar{\mathbf{i}})}\left(\dot{\bar{v}}_{x\mathbf{i}} - \bar{\omega}_{\mathbf{i}}\bar{v}_{y\mathbf{i}}\right) + s_{(\mathbf{i}-\bar{\mathbf{i}})}\left(\dot{\bar{v}}_{y\mathbf{i}} + \bar{\omega}_{\mathbf{i}}\bar{v}_{x\mathbf{i}}\right) \\ &\quad - \lambda_1[v_{x\mathbf{i}} - c_{(\mathbf{i}-\bar{\mathbf{i}})}\bar{v}_{x\mathbf{i}} - s_{(\mathbf{i}-\bar{\mathbf{i}})}\bar{v}_{y\mathbf{i}}] - f_{x\mathbf{i}}(v_{x\mathbf{i}}, v_{y\mathbf{i}}, \omega_{\mathbf{i}}), \end{aligned} \tag{18}$$

$$\tau_{2\mathbf{i}} = u_{2\mathbf{i}} + \dot{\bar{\omega}}_{\mathbf{i}} - \lambda_3(\omega_{\mathbf{i}} - \bar{\omega}_{\mathbf{i}}) - f_{\omega\mathbf{i}}(v_{x\mathbf{i}}, v_{y\mathbf{i}}, \omega_{\mathbf{i}}), \tag{19}$$

we derive the error dynamics in a reduced form

$$\dot{z}_{\mathbf{i}} = \begin{bmatrix} \omega_{\mathbf{i}} z_{2\mathbf{i}} \\ -\omega_{\mathbf{i}} z_{1\mathbf{i}} \\ 0 \end{bmatrix} + \begin{bmatrix} u_{1\mathbf{i}} \\ \Psi_{\mathbf{i}} \\ u_{2\mathbf{i}} \end{bmatrix} + \begin{bmatrix} \delta_{x\mathbf{i}} \\ \delta_{y\mathbf{i}} \\ \delta_{\omega\mathbf{i}} \end{bmatrix}, \tag{20}$$

where $\Psi_{\mathbf{i}}$ is given as

$$\begin{aligned} \Psi_{\mathbf{i}} &= \omega_{\mathbf{i}} v_{x\mathbf{i}} + s_{(\mathbf{i}-\bar{\mathbf{i}})}\left(\dot{\bar{v}}_{x\mathbf{i}} - \bar{\omega}_{\mathbf{i}}\bar{v}_{y\mathbf{i}}\right) - c_{(\mathbf{i}-\bar{\mathbf{i}})}\left(\dot{\bar{v}}_{y\mathbf{i}} + \bar{\omega}_{\mathbf{i}}\bar{v}_{x\mathbf{i}}\right) \\ &\quad + \lambda_2[v_{y\mathbf{i}} + s_{(\mathbf{i}-\bar{\mathbf{i}})}\bar{v}_{x\mathbf{i}} - c_{(\mathbf{i}-\bar{\mathbf{i}})}\bar{v}_{y\mathbf{i}}] + f_{y\mathbf{i}}(v_{x\mathbf{i}}, v_{y\mathbf{i}}, \omega_{\mathbf{i}}). \end{aligned} \tag{21}$$

Therefore, from the discussion above, the formation control problem is converted to design new control inputs $(u_{1\mathbf{i}}, u_{2\mathbf{i}})$ that result in uniformly asymptotically stable error dynamics (20) for all follower vessels $\mathbf{i} = 1, \ldots, N$.

B. Control Design

In this paper, we propose the following nonlinear time-varying controller:

$$u_{1\mathbf{i}} = -k_{1\mathbf{i}} z_{1\mathbf{i}}, \tag{22}$$

$$u_{2\mathbf{i}} = -k_{3\mathbf{i}} z_{3\mathbf{i}} - k_{2\mathbf{i}}\frac{\Psi_{\mathbf{i}}}{z_{3\mathbf{i}}} z_{2\mathbf{i}}, \tag{23}$$

where $k_{1\mathbf{i}}$, $k_{2\mathbf{i}}$ and $k_{3\mathbf{i}}$ are positive control gains, $\Psi_{\mathbf{i}}$ is given by (21). We have the following result.

Lemma 2: If $z_{3\mathbf{i}} \to 0$ exponentially at a rate $\gamma > 0$ as $t \to \infty$ and the control gain $\lambda_1 \geq \gamma$, then $\Psi_i / z_{3\mathbf{i}}$ is bounded.

Proof: It is noted that $z_{3\mathbf{i}} \xrightarrow{\gamma} 0$ implies that $\omega_{\mathbf{i}} - \bar{\omega}_{\mathbf{i}} \xrightarrow{\gamma} 0$ and $\theta_{\mathbf{i}} - \bar{\theta}_{\mathbf{i}} \xrightarrow{\gamma} 0$. Thus, we have $\sin(\theta_{\mathbf{i}} - \bar{\theta}_{\mathbf{i}}) \xrightarrow{\gamma} 0$ and $\cos(\theta_{\mathbf{i}} - \bar{\theta}_{\mathbf{i}}) \xrightarrow{\gamma^2/2} 1$. From (21), we have

$$\begin{aligned} \Psi_{\mathbf{i}} &= \omega_{\mathbf{i}} v_{x\mathbf{i}} - \left(\dot{\bar{v}}_{y\mathbf{i}} + \bar{\omega}_{\mathbf{i}}\bar{v}_{x\mathbf{i}}\right) + \lambda_2(v_{y\mathbf{i}} - \bar{v}_{y\mathbf{i}}) + f_{y\mathbf{i}}(v_{x\mathbf{i}}, v_{y\mathbf{i}}, \omega_{\mathbf{i}}) \\ &= \left(\dot{v}_{y\mathbf{i}} - \dot{\bar{v}}_{y\mathbf{i}}\right) + \bar{\omega}_{\mathbf{i}}\left(v_{x\mathbf{i}} - \bar{v}_{x\mathbf{i}}\right) + \lambda_2\left(v_{y\mathbf{i}} - \bar{v}_{y\mathbf{i}}\right) + o_1(t), \end{aligned}$$

where $o_1(t) \xrightarrow{\gamma} 0$. Then, it follows from the feedback transformation (18) and the vessel model (1b) that

$$\dot{v}_{x\mathbf{i}} - \dot{\bar{v}}_{x\mathbf{i}} = -\lambda_1 (v_{x\mathbf{i}} - \bar{v}_{x\mathbf{i}}) + \bar{\omega}_{\mathbf{i}} \left(v_{y\mathbf{i}} - \bar{v}_{y\mathbf{i}}\right) + o_2(t),$$
$$\dot{v}_{y\mathbf{i}} - \dot{\bar{v}}_{y\mathbf{i}} = \left[f^{\mathrm{C}}_{y\mathbf{i}}(v_{x\mathbf{i}}, \omega_{\mathbf{i}}) - f^{\mathrm{C}}_{y\mathbf{i}}(\bar{v}_{x\mathbf{i}}, \bar{\omega}_{\mathbf{i}})\right] + \left[f^{\mathrm{D}}_{y\mathbf{i}}(v_{y\mathbf{i}}) - f^{\mathrm{D}}_{y\mathbf{i}}(\bar{v}_{y\mathbf{i}})\right]$$

where $o_2(t) \xrightarrow{\gamma} 0$. Thus, from Assumption 1, we have

$$\begin{bmatrix} \dot{\xi}_1 \\ \dot{\xi}_2 \end{bmatrix} = \begin{bmatrix} -\lambda_1 & \bar{\omega}_{\mathbf{i}}(t) \\ -\eta_{\mathbf{i}} \bar{\omega}_{\mathbf{i}}(t) & \mathscr{A}_{22}(t) \end{bmatrix} \begin{bmatrix} \xi_1 \\ \xi_2 \end{bmatrix} + o(t), \tag{24}$$

where $\xi_1 = v_{x\mathbf{i}} - \bar{v}_{x\mathbf{i}}$, $\xi_2 = v_{y\mathbf{i}} - \bar{v}_{y\mathbf{i}}$, $\mathscr{A}_{22}(t) = \partial f_{y\mathbf{i}} / \partial v_{y\mathbf{i}} \leq 0$, and $o(t) \xrightarrow{\gamma} 0$. It follows [22] that $(\xi_1, \xi_2) \xrightarrow{\gamma} 0$, and therefore $\Psi_{\mathbf{i}} \xrightarrow{\gamma} 0$. Since $\Psi_{\mathbf{i}} \to 0$ has the same order as $z_{3\mathbf{i}} \to 0$, we conclude that term $\Psi_{\mathbf{i}}/z_{3\mathbf{i}}$ is bounded. ■

Based on the above analysis, the control laws (22) and (23) are smooth and bounded if the formation error $z_{\mathbf{i}}$ is bounded. Then, under the controller (22) and (23), the error dynamics (20) are transformed into

$$\begin{bmatrix} \dot{z}_{1\mathbf{i}} \\ \dot{z}_{3\mathbf{i}} \\ \dot{z}_{2\mathbf{i}} \end{bmatrix} = \begin{bmatrix} -k_{1\mathbf{i}} & 0 & \omega_{\mathbf{i}} \\ 0 & -k_{3\mathbf{i}} & -k_{2\mathbf{i}} \Psi_{\mathbf{i}}/z_{3\mathbf{i}} \\ -\omega_{\mathbf{i}} & \Psi_{\mathbf{i}}/z_{3\mathbf{i}} & 0 \end{bmatrix} \begin{bmatrix} z_{1\mathbf{i}} \\ z_{3\mathbf{i}} \\ z_{2\mathbf{i}} \end{bmatrix} + \begin{bmatrix} \delta_{x\mathbf{i}} \\ \delta_{\omega\mathbf{i}} \\ \delta_{y\mathbf{i}} \end{bmatrix}. \tag{25}$$

Our main result is the following.

Theorem 1: Consider a group of heterogeneous planar underactuated vehicles with the communication topology graph $\mathscr{G}$, the node dynamics given by equations (1a), (1b), and the error dynamics given by (20).

(i.) If the disturbance terms $\delta_{x\mathbf{i}}, \delta_{y\mathbf{i}}, \delta_{\omega\mathbf{i}}$ are vanishing with respect to $z_{\mathbf{i}}$, then under the control laws (18), (19), (22) and (23) with positive control gains $\lambda_1, \lambda_2, \lambda_3$ $k_{1\mathbf{i}}, k_{2\mathbf{i}}$ and $k_{3\mathbf{i}}$, where $k_{1\mathbf{i}} \geq k_{3\mathbf{i}}/k_{2\mathbf{i}}$, the origin of the error dynamics (25) is uniformly globally asymptotically stable.

(ii.) Furthermore, if all disturbance terms $\delta_{x\mathbf{i}}, \delta_{y\mathbf{i}}$, and $\delta_{\omega\mathbf{i}}$ are bounded such that $|\delta_{x\mathbf{i}}|_\infty \leq \Delta_{x\mathbf{i}}, |\delta_{y\mathbf{i}}|_\infty \leq \Delta_{y\mathbf{i}}, |\delta_{\omega\mathbf{i}}|_\infty \leq \Delta_{\omega\mathbf{i}}$, then the solutions of the error dynamics (25) is globally uniformly ultimately bounded.

Proof: (i.) Consider the Lyapunov function candidate for the error dynamics (25) as $V(z_{\mathbf{i}}) = \frac{1}{2}\left(z_{1\mathbf{i}}^2 + z_{2\mathbf{i}}^2 + \frac{1}{k_{2\mathbf{i}}} z_{3\mathbf{i}}^2\right)$. It follows that, along the trajectories of (25), we have

$$\dot{V}(z_{\mathbf{i}}(t)) = -k_{1\mathbf{i}} z_{1\mathbf{i}}^2 - k_{3\mathbf{i}} z_{3\mathbf{i}}^2 / k_{2\mathbf{i}} \leq 0, \tag{26}$$

which implies that the closed-loop system is globally uniformly stable, and thus the formation error $z_{\mathbf{i}}$ is bounded over the time interval $[0, +\infty)$. Furthermore, from LaSalle-Yoshizawa Theorem, and by integrating both sides of (26), we can conclude that both $z_{1\mathbf{i}}$ and $z_{3\mathbf{i}}$ converge to zero exponentially with convergence rates $k_{1\mathbf{i}}$ and $k_{3\mathbf{i}}/k_{2\mathbf{i}}$, respectively. Then, from Lemma 2, all terms in (25) are bounded. Moreover, from the convergence of $\omega_{\mathbf{i}} - \bar{\omega}_{\mathbf{i}} \to 0$, and the PE assumption of reference trajectory (7), either $\omega_{\mathbf{i}}(t)$ or $-k_{2\mathbf{i}} \Psi_{\mathbf{i}}/z_{3\mathbf{i}}$ is PE, then the origin of (25) is uniformly globally asymptotically stable [22].

(ii.) In the case of bounded disturbances, it follows from the converse Lyapunov theorem and the boundedness of disturbance terms that the solutions of the error dynamics (25) are globally uniformly ultimately bounded. ■

IV. Simulation Results

Consider a heterogeneous surface vessel network. We assume that $\Omega_{\mathbf{1}} = \{\mathbf{0}\}$ and $\Omega_{\mathbf{2}} = \{\mathbf{0}, \mathbf{1}\}$ and set the weighting coefficients

$$w_{\mathbf{10}} = 1, w_{\mathbf{20}} = 0.8, w_{\mathbf{21}} = 0.2.$$

We assume that the agents **0** and **1** are identical vessels, which are modeled with diagonal mass matrix and linear hydrodynamic damping [12], that is

$$f_{x\mathbf{i}} = \frac{m_{22,\mathbf{i}}}{m_{11,\mathbf{i}}} v_{y\mathbf{i}} \omega_{\mathbf{i}} - \frac{d_{11,\mathbf{i}}}{m_{11,\mathbf{i}}} v_{x\mathbf{i}},$$
$$f_{y\mathbf{i}} = -\frac{m_{11,\mathbf{i}}}{m_{22,\mathbf{i}}} v_{x\mathbf{i}} \omega_{\mathbf{i}} - \frac{d_{22,\mathbf{i}}}{m_{22,\mathbf{i}}} v_{y\mathbf{i}},$$
$$f_{\omega\mathbf{i}} = \frac{m_{11,\mathbf{i}} - m_{22,\mathbf{i}}}{m_{33,\mathbf{i}}} v_{x\mathbf{i}} v_{y\mathbf{i}} - \frac{d_{33,\mathbf{i}}}{m_{33,\mathbf{i}}} \omega_{\mathbf{i}},$$

and the parameters in SI unites are given as

$$m_{11,\mathbf{i}} = 1.412,\ m_{22,\mathbf{i}} = 1.982,\ m_{33,\mathbf{i}} = 0.354$$
$$d_{11,\mathbf{i}} = 3.436,\ d_{22,\mathbf{i}} = 12.99,\ d_{33,\mathbf{i}} = 0.864.$$

Vessel **2** is modeled with diagonal mass matrix but nonlinear hydrodynamic damping [14], that is

$$f_{x\mathbf{i}} = \frac{m_{22,\mathbf{i}}}{m_{11,\mathbf{i}}} v_{y\mathbf{i}} \omega_{\mathbf{i}} - \frac{d_{11,\mathbf{i}}}{m_{11,\mathbf{i}}} |v_{x\mathbf{i}}|^{\alpha_{11,\mathbf{i}}} \operatorname{sign}(v_{x\mathbf{i}}),$$
$$f_{y\mathbf{i}} = -\frac{m_{11,\mathbf{i}}}{m_{22,\mathbf{i}}} v_{x\mathbf{i}} \omega_{\mathbf{i}} - \frac{d_{22,\mathbf{i}}}{m_{22,\mathbf{i}}} \left|v_{y\mathbf{i}}\right|^{\alpha_{22,\mathbf{i}}} \operatorname{sign}\left(v_{y\mathbf{i}}\right),$$
$$f_{\omega\mathbf{i}} = \frac{m_{11,\mathbf{i}} - m_{22,\mathbf{i}}}{m_{33,\mathbf{i}}} v_{x\mathbf{i}} v_{y\mathbf{i}} - \frac{d_{33,\mathbf{i}}}{m_{33,\mathbf{i}}} |\omega_{\mathbf{i}}|^{\alpha_{33,\mathbf{i}}} \operatorname{sign}(\omega_{\mathbf{i}}),$$

where the parameters in SI unites are given as

$$m_{11,\mathbf{2}} = 1.317,\ m_{22,\mathbf{2}} = 3.832,\ m_{33,\mathbf{2}} = 0.926$$
$$d_{11,\mathbf{2}} = 5.252,\ d_{22,\mathbf{2}} = 14.138,\ d_{33,\mathbf{2}} = 2.262$$
$$\alpha_{11,\mathbf{2}} = 1.510,\ \alpha_{22,\mathbf{2}} = 1.747,\ \alpha_{33,\mathbf{2}} = 1.592.$$

In this simulation, the leader vessel is commanded to follow a U-shape trajectory, and the geometric shape of the desired formation for the three vehicles is a triangle configuration, i.e., $\left[d^1_{\mathbf{10}}, d^2_{\mathbf{10}}\right] = [-1 \text{ m}, -1 \text{ m}]$ and $\left[d^1_{\mathbf{20}}, d^2_{\mathbf{20}}\right] = [1 \text{ m}, -1 \text{ m}]$, as shown in Fig. 2. All vehicles start from rest. The initial poses for the three vehicles in SI units are given as follows:

$$q^0_{\mathbf{0}} = [0, 0, \pi/2]^\top,\ q^0_{\mathbf{1}} = [-1.5, -1, 0]^\top,\ q^0_{\mathbf{2}} = [-2, -2, 0]^\top.$$

The control gains were selected as

$$\lambda_1 = \lambda_2 = \lambda_3 = 2,$$
$$k_{1\mathbf{i}} = 3,\ k_{2\mathbf{i}} = k_{3\mathbf{i}} = 1,\ \mathbf{i} = 1, 2.$$

The simulation results are shown in Figs. 2 and 3. Figure 2 shows the paths of the three vessels in the formation where the desired triangular geometry is achieved after approximately 60 seconds. The configuration error trajectories of the two follower vessels are shown in Fig. 3. The convergence of the configuration formation error trajectories implies that the error dynamics is stabilized in approximately 60s.

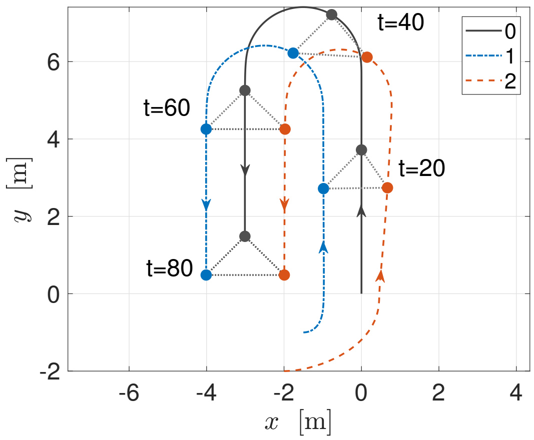

Fig. 2. Illustration of the paths of the three surface vessels in formation.

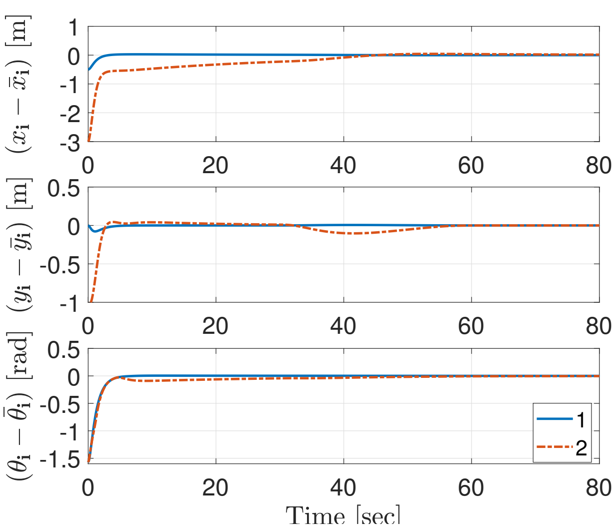

Fig. 3. Trajectories of the configuration errors of the surface vessels in the network.

V. Conclusion

In this work, we present a new singularity-free decentralized formation tracking control framework for heterogeneous underactuated surface vessels. The approach is based on leader-follower model relying on relative coordination and thus without requiring any global position measurements. Using the cascade structure of vehicle dynamic model, a transformation is proposed to reduce the order of error dynamics, and then the smooth time-varying controller is developed with the aid of Lyapunov method and only relies on the assumption that either the surge or yaw reference velocity is persistently exciting. The proposed controller guarantees uniform global asymptotic stability and strong robustness properties in the formation-error-coordinates space, and can be implemented in directed time-invariant communication networks with a spanning tree. Our future research will concentrate on formation control of surface vessels and other types of vehicles, such as mobile robots and aircraft.

References

[1] F. Fahimi, "Sliding-mode formation control for underactuated surface vessels," *IEEE Transactions on Robotics*, vol. 23, no. 3, pp. 617–622, 2007.

[2] F. Arrichiello, S. Chiaverini, and T. I. Fossen, "Formation control of underactuated surface vessels using the null-space-based behavioral control," in *2006 IEEE/RSJ International Conference on Intelligent Robots and Systems*. IEEE, 2006, pp. 5942–5947.

[3] M. A. Lewis and K.-H. Tan, "High precision formation control of mobile robots using virtual structures," *Autonomous robots*, vol. 4, no. 4, pp. 387–403, 1997.

[4] L. Consolini, F. Morbidi, D. Prattichizzo, and M. Tosques, "Leader–follower formation control of nonholonomic mobile robots with input constraints," *Automatica*, vol. 44, no. 5, pp. 1343–1349, 2008.

[5] W. Dong and J. A. Farrell, "Formation control of multiple underactuated surface vessels," *IET Control Theory & Applications*, vol. 2, no. 12, pp. 1077–1085, 2008.

[6] W. Dong, "Cooperative control of underactuated surface vessels," *IET control theory & applications*, vol. 4, no. 9, pp. 1569–1580, 2010.

[7] K. D. Do, "Practical formation control of multiple underactuated ships with limited sensing ranges," *Robotics and Autonomous Systems*, vol. 59, no. 6, pp. 457–471, 2011.

[8] X. Jin, "Fault tolerant finite-time leader–follower formation control for autonomous surface vessels with los range and angle constraints," *Automatica*, vol. 68, pp. 228–236, 2016.

[9] J. Ghommam and M. Saad, "Adaptive leader–follower formation control of underactuated surface vessels under asymmetric range and bearing constraints," *IEEE Transactions on Vehicular Technology*, vol. 67, no. 2, pp. 852–865, 2017.

[10] Z. Sun, G. Zhang, Y. Lu, and W. Zhang, "Leader-follower formation control of underactuated surface vehicles based on sliding mode control and parameter estimation," *ISA transactions*, vol. 72, pp. 15–24, 2018.

[11] T. Li, R. Zhao, C. P. Chen, L. Fang, and C. Liu, "Finite-time formation control of under-actuated ships using nonlinear sliding mode control," *IEEE Transactions on Cybernetics*, vol. 48, no. 11, pp. 3243–3253, 2018.

[12] Z.-P. Jiang, "Global tracking control of underactuated ships by lyapunov's direct method," *Automatica*, vol. 38, no. 2, pp. 301–309, 2002.

[13] E. Lefeber, K. Y. Pettersen, and H. Nijmeijer, "Tracking control of an underactuated ship," *IEEE transactions on control systems technology*, vol. 11, no. 1, pp. 52–61, 2003.

[14] H. Ashrafiuon, S. Nersesov, and G. Clayton, "Trajectory tracking control of planar underactuated vehicles," *IEEE Trans. Automat. Contr.*, vol. 62, no. 4, pp. 1959–1965, 2017.

[15] B. Wang, S. Nersesov, and H. Ashrafiuon, "A unified approach to stabilization, trajectory tracking, and formation control of planar underactuated vehicles," in *2020 American Control Conference (ACC)*. IEEE, 2020, pp. 5269–5274.

[16] M. A. Maghenem, A. Loria, and E. Panteley, "Cascades-based leader-follower formation-tracking and stabilization of multiple nonholonomic vehicles," *IEEE Trans. Automat. Contr.*, 2019.

[17] M. Ghasemi and S. G. Nersesov, "Finite-time coordination in multiagent systems using sliding mode control approach," *Automatica*, vol. 50, no. 4, pp. 1209–1216, 2014.

[18] K. D. Do and J. Pan, "Global tracking control of underactuated ships with nonzero off-diagonal terms in their system matrices," *Automatica*, vol. 41, no. 1, pp. 87–95, 2005.

[19] H. Ashrafiuon, K. R. Muske, L. C. McNinch, and R. A. Soltan, "Sliding-mode tracking control of surface vessels," *IEEE Trans. Ind. Electron.*, vol. 55, no. 11, pp. 4004–4012, 2008.

[20] J.-H. Li, P.-M. Lee, B.-H. Jun, and Y.-K. Lim, "Point-to-point navigation of underactuated ships," *Automatica*, vol. 44, no. 12, pp. 3201–3205, 2008.

[21] C. A. Desoer and M. Vidyasagar, *Feedback systems: input-output properties*. Siam, 1975.

[22] A. Loria and E. Panteley, "Uniform exponential stability of linear time-varying systems: revisited," *Systems & Control Letters*, vol. 47, no. 1, pp. 13–24, 2002.